Some notes on bathymetric effects in marine magnetotellurics, motivated by an amphibious experiment at the South Chilean margin

Gerhard Kapinos, Heinrich Brasse [1]
Freie Universität Berlin, Fachrichtung Geophysik, Malteserstr. 74-100, 12249 Berlin, Germany

1 Introduction

Whilst the onshore magnetotelluric method is established as a useful method for imaging electrical conductivity structures in the deep earth's interior, electromagnetic investigation in marine environment has attracted until recently much less attention, although the oceans cover the most part of the Earth's surface. Beside of logistical challenges, high technical demands on the instruments and involved higher costs, physical conditions in marine environments make the acquisition and interpretation of offshore data by far more difficult than onshore data. The broad period range of usable signals utilized in the terrestrial MT is substantially limited on the seafloor. The ionospheric and magnetospheric primary source field recorded on the seafloor is at short periods strongly attenuated by the covering highly conductive ocean layer and at long periods contaminated by motionally induced secondary electromagnetic fields. Additionally, attention has to be payed to the shape of the ocean bottom, which can massively distort the electromagnetic fields particularly in coast region.

2 Decay of electromagnetic fields in the ocean

The decay of the electromagnetic amplitude in a high conductive homogeneous half space like ocean water ($\rho = 0.3\Omega m$) and a less conductive medium like earth ($\rho = 100\Omega m$) shows Fig. 1. In a homogeneous half space without boundary in vertical direction the field behaviour in both media can be estimated according to the simple formula used for the calculation of the skin depth

$$\vec{F} = \vec{F_0} e^{-kz}, \tag{1}$$

[1] kapinosg@geophysik.fu-berlin.de, h.brasse@geophysik.fu-berlin.de

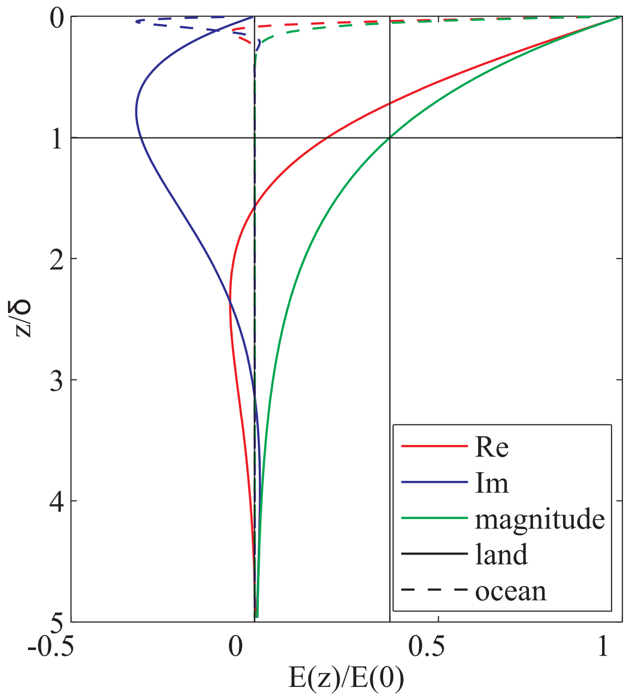

Figure 1: Decay of the of magnitude of electromagnetic field $\vec{F}$ (green) and its real (red) and imaginary part (blue) as function of depth in a highly conductive (i.e. ocean water, dashed line) and a less conductive homogeneous half space (solid line). The decay is scaled to the surface value $\vec{F}_0$.

where $k = \sqrt{i\mu\sigma\omega}$. At a depth of 4000 m, which corresponds to the average ocean depth, the amplitude of a field propagating in the ocean at a period of 10 s is attenuated hundredfold, i.e. the field on the ocean bottom would be approximately 1% of the surface value.

This simple relationship becomes more complicated when taking into account real conditions with a highly conductive ocean layer which is limited downward by a relatively resistive basement. Analog to the N-layered half space the solution has to be upgraded by a further term according to the reflection on the ocean bottom at depth h. The solution for the x-component of the electric field in the first and second layer is

$$E_{1,x} = E_{11}e^{-k_1 z} + E_{12}e^{k_1 z} \quad (2)$$

$$E_{2,x} = E_{22}e^{-k_2 z} \quad (3)$$

where E_{11} is the amplitude of the downgoing and E_{12} of the upgoing wave in the first medium and E_{22} the amplitude of the downgoing wave in the second medium. For the $y-$component of the magnetic field follows from *Faraday's law* in a 1-D case

$$B_{1,y} = -\frac{1}{i\omega}\frac{\partial E_{1x}}{\partial z} = \frac{k_1}{i\omega}\left(E_{11}e^{-k_1 z} - E_{12}e^{k_1 z}\right) \quad (4)$$

$$B_{2,y} = -\frac{1}{i\omega}\frac{\partial E_{2x}}{\partial z} = \frac{k_2}{i\omega}E_{22}e^{-k_2 z}. \quad (5)$$

A similar relation can be derived for the pair E_y and B_x. Using the continuity of the fields at $z = h$ resulting from the boundary conditions

$$E_{1,x}(h) = E_{2,x}(h), \qquad B_{1,y}(h) = B_{2,y}(h) \tag{6}$$

and introducing the admittances

$$\zeta_1 = \frac{k_1}{i\omega} = \sqrt{\frac{i\omega\mu\sigma_1}{i\omega}} = \sqrt{\frac{\mu\sigma_1}{i\omega}} \qquad \textit{and} \qquad \zeta_2 = \frac{k_2}{i\omega} = \sqrt{\frac{\mu\sigma_2}{i\omega}} \tag{7}$$

the ratio of amplitudes of the downgoing and upgoing fields in the ocean is

$$\frac{E_{12}}{E_{11}} = \frac{\zeta_1 - \zeta_2}{\zeta_1 + \zeta_2} e^{-2k_1 h} = \zeta_{12} e^{-2k_1 h}, \tag{8}$$

where $\zeta_{12} = \frac{\zeta_1 - \zeta_2}{\zeta_1 + \zeta_2}$ is the reflection coefficient. Its value is estimated according to eq. 7 by the conductivity contrast at the boundary between layers. For instance, in case of sharp contrast like ocean water ($\sigma_1 = 3.2\, S/m$) and basement ($\sigma_2 = 0.001\, S/m$) $\zeta_{12} = 0.965$. Note, that using as solution in eq. 2 and 3 the magnetic field instead of electric field, the reflection coefficient has to be expressed by reciprocal impedances instead of admittance and yields: $\eta_{12} = \frac{\eta_1 - \eta_2}{\eta_1 + \eta_2}$, with $\eta_{1,2} = \frac{k_1}{\mu\sigma_{1,2}} = \sqrt{\frac{i\omega}{\mu\sigma_{1,2}}}$.
Combining the equations 8 and 2 the electric field at depth $z \leq h$ becomes

$$E_{1,x}(z) \;=\; E_{11}\left(e^{-k_1 z} + \zeta_{12} e^{-2k_1 h} e^{k_1 z}\right) \tag{9}$$

and at the surface $z = 0$

$$E_{1,x}(0) \;=\; E_{11}\left(1 + \zeta_{12} e^{-2k_1 h}\right). \tag{10}$$

The ratio of the equations 9 and 10 gives the attenuation of the electric field in the ocean for $0 \leq z \leq h$ normalized in terms of the total field at the surface

$$|V_E| = \frac{E_{1,x}(z)}{E_{1,x}(0)} \;=\; \frac{e^{-k_1 z} + \zeta_{12} e^{-2k_1 h}}{1 + \zeta_{12} e^{-2k_1 h}} = \frac{1 + \zeta_{12} e^{-2k_1 (h-z)}}{1 + \zeta_{12} e^{-2k_1 h}} e^{-k_1 z} \tag{11}$$

This applies accordingly for the ratio of magnetic fields

$$B_{1,y}(z) \;=\; B_{11}\zeta_1\left(e^{-k_1 z} - \zeta_{12} e^{-2k_1 h} e^{k_1 z}\right) \tag{12}$$

$$B_{1,y}(0) \;=\; B_{11}\zeta_1\left(1 - \zeta_{12} e^{-2k_1 h}\right) \tag{13}$$

$$|V_B| = \frac{B_{1,y}(z)}{B_{1,y}(0)} \;=\; \frac{e^{-k_1 z} - \zeta_{12} e^{-2k_1 h}}{1 - \zeta_{12} e^{-2k_1 h}} = \frac{1 - \zeta_{12} e^{-2k_1 (h-z)}}{1 - \zeta_{12} e^{-2k_1 h}} e^{-k_1 z}. \tag{14}$$

The behaviour of the electric and magnetic fields as function of depth in a 5 km deep ocean for two selected and representative periods (100 s and 10000 s) and realistic conductivities in the ocean ($\sigma_1 = 3.2\,\mathrm{S/m}$) and basement ($\sigma_1 = 0.001\,\mathrm{S/m}$) is illustrated in Fig. 2(left). The fields are normalized to their surface magnitude according to relations

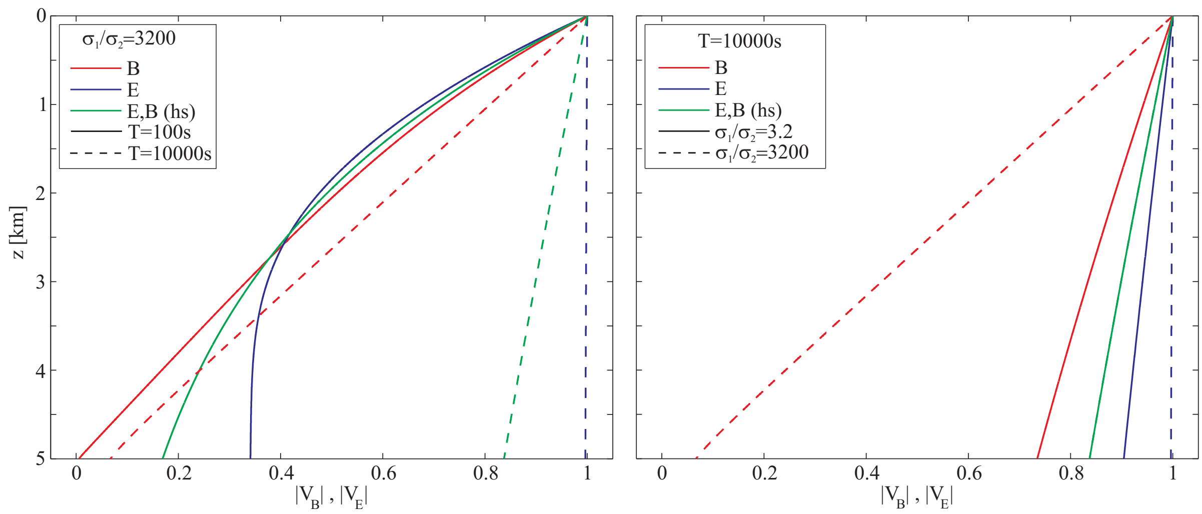

Figure 2: The decay of electromagnetic fields in an ocean shows a deviation from simple half space attenuation due to boundary conditions on the seafloor and depends beside period length and ocean depth also on resistivity contrast between ocean water and basement. Attenuation of electric (blue) and magnetic (red) fields for two periods $T_1 = 100\,s$ (solid line) and $T_1 = 10000\,s$ (dashed line) in a 5 km deep ocean with a sea water resistivity of $0.3\,\Omega m$ and seafloor resistivity of $1000\,\Omega m$(right). Attenuation of the fields at a period of $10000\,s$ for two different conductivities of the basement (0.001 S/m and 1 S/m) (left). See also (Brasse, 2009).

11 and 14. They show different decay in dependence of period. At short periods (solid line) both the electric (blue) and magnetic (red) fields experience strong attenuation and the curve shape is determined by exponential decay. Large differences in attenuation are observed at long periods (dashed line). While the electric field penetrates the ocean layer from surface to the seafloor nearly unchanged, the magnetic field is attenuated about fifteen-fold and reaches on the ocean bottom just about 7% of its surface value. However, both fields would behave identically in an infinitely extended ocean, that would be regarded as a homogeneous half space.

At first sight of the equations 11 and 14 one would think that the behaviour of the fields depends rather on the ocean thickness than on period. However, actually both is true. The decay of the fields is determined by both period T and thickness h of the ocean layer. That becomes evident considering the exponential and crucial term in the equations as function of skin depth according to the relations of skin depth $\delta = \sqrt{\frac{2}{\omega\sigma\mu}}$ and complex wave number $k = (1+i)\sqrt{\frac{\omega\sigma\mu}{2}}$:

$$e^{-2k_1 h} = e^{-\frac{2h}{\delta_1}(i+1)}. \tag{15}$$

The quantity $\frac{h}{\delta_1}$ is the electrical layer thickness and via $\delta \sim \sqrt{T}$ also directly associated with the period length of the penetrating wave (McNeill and Labson, 1986). The fields behave identically if the exponent remains constant, regardless if high frequency fields propagate in a shallow ocean or low frequency fields in a deep ocean. The behaviour of the fields replicates, similar to a self-similarity principle by stimulating the exponent

$\frac{h}{\delta_1}$, i.e. by appropriate and simultaneous increasing or decreasing the frequency and the ocean thickness and thus creating either electrical thick $\frac{h}{\delta_1} >> 1$ or thin conditions $\frac{h}{\delta_1} << 1$. In real world an electrical thick layer is equal to a high frequency field where the thickness of the ocean is much larger than the skin depth $\frac{h}{\delta_1} >> 1$ and both $e^{-2k_1 h}$ and $e^{-2k_1(h-z)} \rightarrow 0$ (Brasse, 2009). Thus the effect of the basement on the fields is only marginal and the behaviour in a thick electrical layer is governed by exponential decay

$$\frac{E_{1,x}(z)}{E_{1,x}(0)} \approx e^{-k_1 z} \quad \text{respectively} \quad \frac{B_{1,y}(z)}{B_{1,y}(0)} \approx e^{-k_1 z}. \tag{16}$$

The decay of both fields becomes more alike the more the ocean depth or the frequency increases until finally approaching the decay curve of a homogeneous half space.

For low frequencies or for an electrically thin ocean, where the skin depth is significantly greater than ocean depth, $\frac{h}{\delta_1} << 1$, the exponential terms can be expanded into a power series

$$e^{\mp cx} \approx 1 \mp cx \qquad (c \in C) \tag{17}$$

Assuming additionally a non-conductive basement so that $\zeta_{12} = 1$ and substituting this approximations into eq. 11 it yields for an electric field

$$\frac{E_{1,x}(z)}{E_{1,x}(0)} = \frac{1 + e^{-2k_1(h-z)}}{1 + e^{-2k_1 h}} e^{-k_1 z} = \frac{1 - k_1(h-z)}{1 - k_1 h}(1 - k_1 z) \tag{18}$$

In the ocean layer at depth $z = h$

$$\frac{E_{1,x}(z)}{E_{1,x}(0)} = \frac{1}{1 - k_1 h}(1 - k_1 z) = 1 \tag{19}$$

and thus the electric field remains constant throughout the ocean as shown in Fig. 2. In this case the current density $J_x = \sigma E_x$ is constant as well.

Another behavior shows the magnetic field in an electrical thin layer. Assuming again an infinite conductivity contrast, $\zeta_{12} = 1$ and the equation 14 yields at $z = h$

$$\frac{B_{1,y}(z)}{B_{1,y}(0)} = \frac{1 - e^{-2k_1(h-z)}}{1 - e^{-2k_1 h}} e^{-k_1 z} = \frac{2k_1(h-z)}{2k_1 h}(1 - k_1 z) = \frac{(h-z)}{h}(1 - k_1 z) = 0 \tag{20}$$

Taking into account a lower conductivity contrast between ocean and basement, the reflection coefficient $\zeta_{12} < 1$ and the calculated attenuation values of the fields don't correspond exactly to the observed decay in Fig. 2(right). Especially the decay of the magnetic field doesn't converge to zero as to be expected from Fig. 2. The attenuation is smaller the larger the wave period and less the conductivity contrast. The first can be considered in terms of skin depth and thus as an effect of electrical thin ocean layer. The second is related to the current distribution in the ocean and the seafloor. According to Ohm's law, $\vec{j} = \sigma\vec{E}$ the current density is much higher in the conductive ocean than in the resistive basement. In the theoretical case of infinitely resistive basement it would imply that the currents only flow in the ocean, inducing a secondary magnetic field which removes entirely the opposite primary field in agreement with the above mentioned result. In real conditions with high but not infinite basement resistivity the currents diffuse also to the seafloor, so that the the secondary magnetic field of the diminished currents in the ocean can in fact reduce but not completely cancel the primary magnetic field. Thus the ratio $\frac{B_{1,y}(z)}{B_{1,y}(0)}$ doesn't become zero rather $0 < \frac{B_{1,y}(z)}{B_{1,y}(0)} < 1$ depending on ζ_{12} and electrical conditions of the ocean layer. In other words the reflection coefficient regularizes the conditions for distribution of electrical currents in sea bottom and estimates in this manner the damping behaviour of the fields (Chave et al., 1991).

The decay of the electric field in the ocean is against intuition, and negligible compared to the magnetic field. In the theoretical case with infinite conductivity contrast, ($\zeta_{12} = 1$) the ocean represents for long periods an electrical thin layer that the electric field passes almost intact. In real condition mentioned above ζ_{12} is still high and the low frequency field decays gently, in terms of an electrical thin layer. That would change assuming a layer of highly conductive sediments on the ocean bottom. Since the layer becomes thicker, the electric field decays more strongly, the magnetic field in contrast much less since a part of currents now flows in the sediments. Thus both fields would approximate the curve of attenuation in a homogeneous half space, what for short periods corresponds to exponential decay Fig. 2(right).

Similar effects would be observed considering the fields at a fixed point z_1, within the ocean ($0 < z_1 < h_1$) as a function of ocean depth. As the ocean depth increases from h_1 to h_2 at a constant period both fields behave differently at a fixed point z_1: the electric field becomes smaller and the magnetic field larger. Again, in deeper ocean currents flow through a broader region, the density becomes smaller as well as the compensating effect of the secondary opposite magnetic field at depth h_1 and the magnetic field increases compared to flat ocean. On the other hand the electric field experiences more attenuation due to the increased electrical layer.

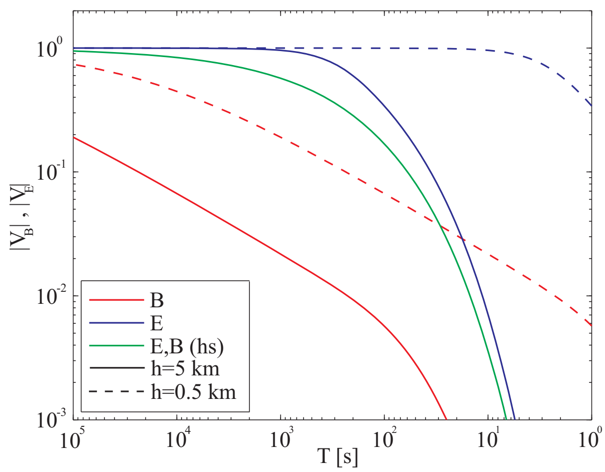

Figure 3: Magnitude of B- and E-fields at the seafloor in 0.5 km depth and 5 km as function of period. In comparison the bahavior of the fields in depth of 5 km in a downward unlimited ocean (homogeneous half space).

It is also instructive to consider the electric and magnetic fields in the ocean as function of periods. Fig. 3 illustrates graphically the ratio $|V_B| = \frac{B_{1,y}(z)}{B_{1,y}(0)}$ and $|V_E| = \frac{E_{1,x}(z)}{E_{1,x}(0)}$ for various thicknesses of the ocean layer. It becomes clear immediately that in the real ocean environment attenuation of the fields differs fundamentally over a total period range. While the electric field remains nearly unchanged in electric thin layer ($\frac{h}{\delta_1} << 1$), i.e. when the skin depth exceeds the ocean thickness, the magnetic field experiences marked attenuation over the total period range, up to about hundredfold of the electric field attenuation. As expected, the range of periods over which the fields decay exponentially increases, when the depth of the ocean increases or the resistivity of the basement diminishes. In the limit case if ($\zeta_{12} = 0$) and the currents flow through an unlimited broad region the curves approximate the decay of a homogeneous half space.

Note that in case of reverse conditions, i.e. the upper layer is more resistive than the lower layer – like may be the case on land – the fields behave reversely as well: the electric field decays quickly while the magnetic field passes the layer almost unchanged.

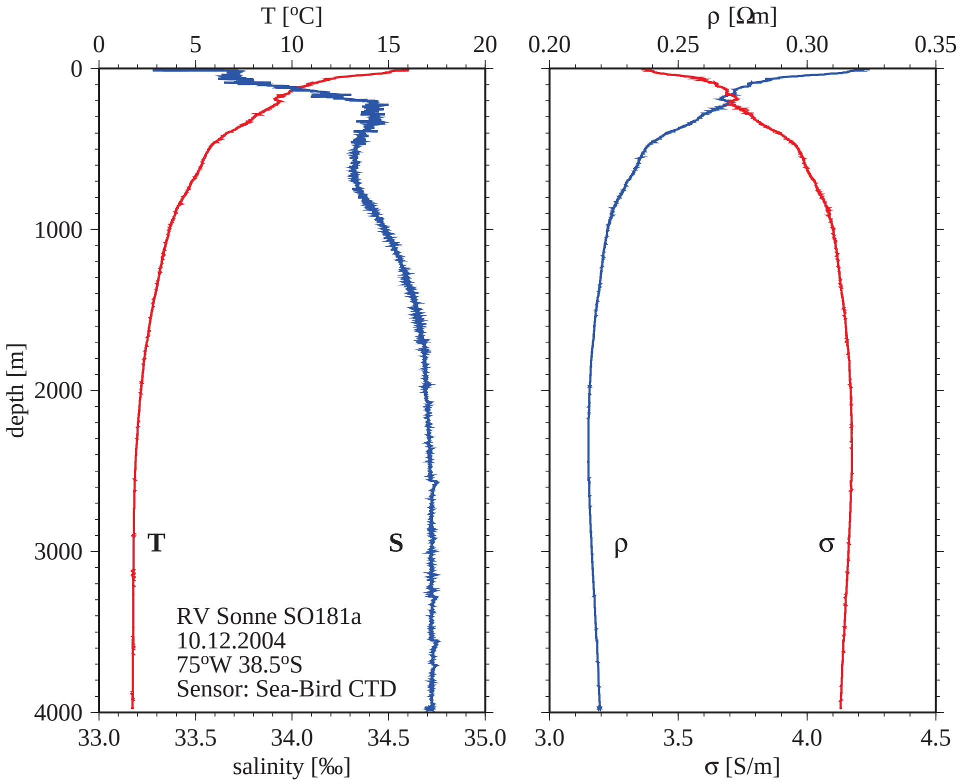

Figure 4: Logs of temperature and salinity (left), electrical conductivity, resistivity (right) measured during RV Sonne leg SO-181.

The resistivity values of the ocean assumed in prior theoretical consideration was motivated by a CTD log performed in 2004 close to the South Chilean continental margin during RV Sonne leg SO-181 at depths until 4000 m (Fig. 4). The knowledge of water conductivity is also essential for subsequent modeling where the ocean has to be incorporated as an a priori structure in the finite difference mesh. The conductivity in ocean depends on pressure, salinity and temperature. While the effect of pressure and salinity is marginally, the temperature variations in ocean change resistivity of oceanic water from 0.16 Ωm at 30°C to 0.33 Ωm at 1.0°C. The estimated resistivity values about 0.3 Ωm corresponds very well to literature values (Filloux, 1987)

3 Offshore magnetotelluric and magnetic transfer functions in presence of bathymetry

The discussions about magnetotellurics on the seafloor are often dominated by attenuation of electromagnetic fields by high conductive ocean and secondary induction by sea tides. Fewer studies refer to distorting effects on electromagnetic fields caused by changes in seafloor bathymetry in presence of overlaying high conductive environment (Constable et al., 2009).

For a model incorporating a homogeneous half space with resistivity of 100Ωm and conductive ocean with bathymetry that is observed at the South Chilean continental margin (Fig. 5, top), magnetotelluric transfer function were calculated with the algorithm of Mackie et al. (1994). At least two clear findings can be derived from the model

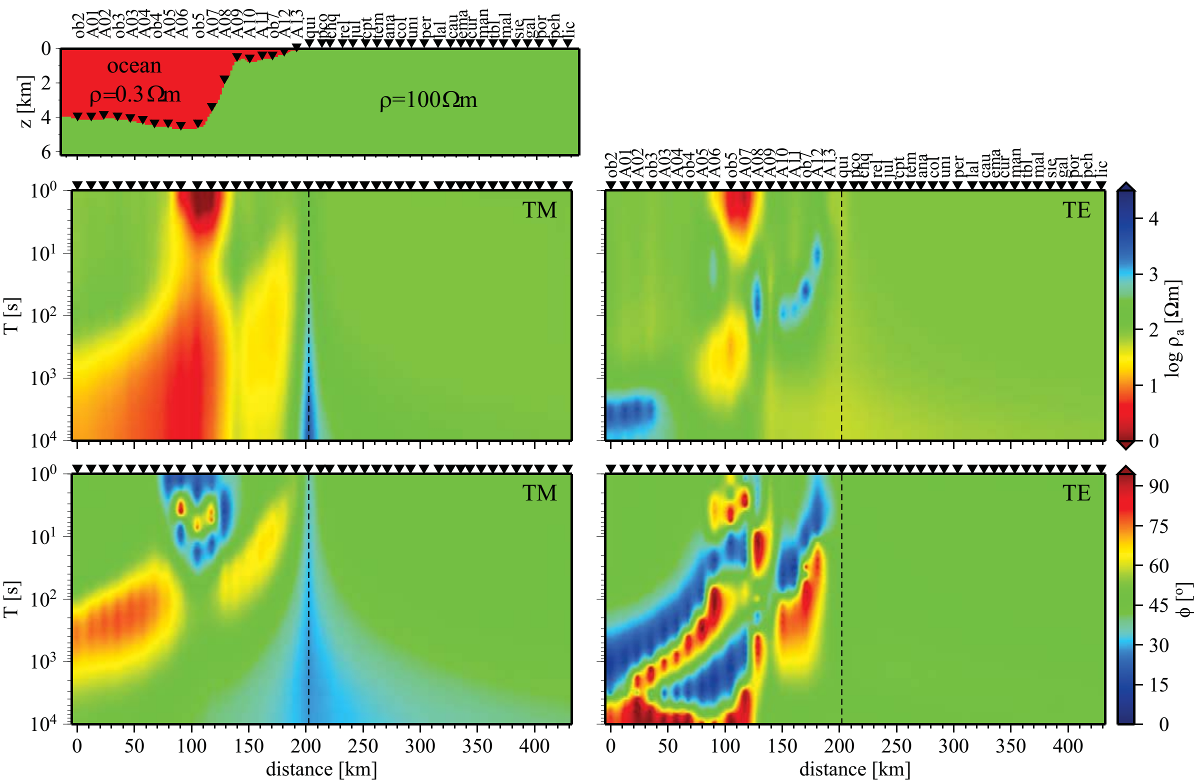

Figure 5: Responses of a synthetic amphibious model shown on the top. Middle: resistivity of TM and TE mode. Bottom: phase of TM and TE mode. Dashed line separates the profile into offshore and onshore part.

responses (Fig. 5, middle and bottom). Firstly the ocean has rather a marginal effect on the onshore magnetotelluric transfer function (right of the dashed line). Actually only in TM mode of onshore stations close to the ocean slightly decreasing phases and enhanced apparent resistivity on the edge between offshore- and onshore profile marked by a dashed line, can be observed. Secondly the bathymetry produces dramatic anomalous effects in the ocean, which can be observed in both modes as well as in phases and resistivities. The resistivity in TE mode rises and falls dramatically producing cusps in the image and phases even exceed $-180°$ and $180°$.

Similar anomalous features can be observed in the magnetic transfer functions (Fig. 6). Slight changes in the shape of the seafloor, adumbrated by a dotted line, are overdrawn reproduced by dramatic variations in the magnitude of the induction arrows (note the smooth bathymetry change between stations A09 and A13 and their huge impact on the magnitude of the induction arrows). On the other hand, the ocean effect on onshore station is limited to long-periods and to near-coastal region, again.

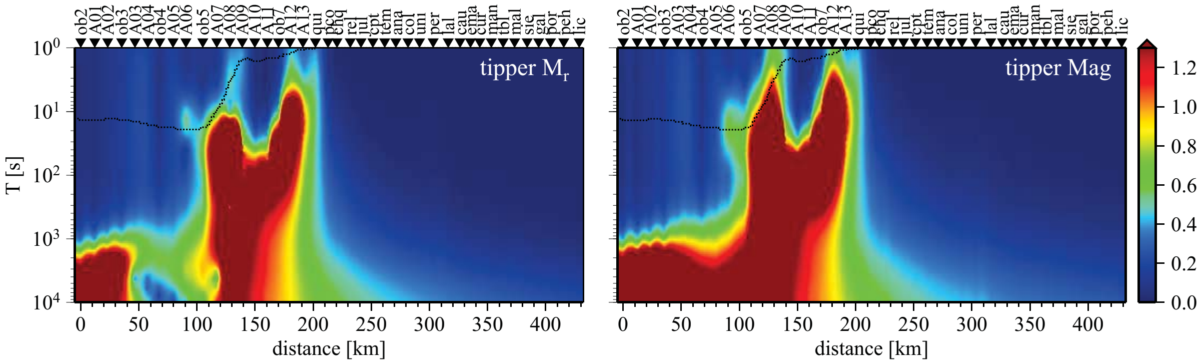

Figure 6: Real part (left) and the magnitude (right) of the tipper calculated for synthetic and amphibious model shown on the top of figure 5. The dotted line indicates the shape of the bathymetry of the model.

Comparing these synthetic responses with the real induction vectors observed at the only station at the continental slope, ob7, shows that the bathymetry indeed affects the measured data, as shown in Fig. 7. The huge induction vectors (over 1) at middle and long periods correspond roughly with magnitude values calculated from the simple amphibious model. For short periods (until 100 s) a comparison is impossible due to

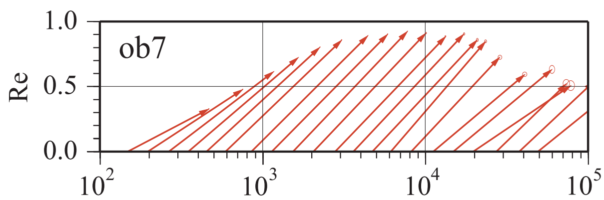

Figure 7: Real part of the observed induction vectors at station ob7, deployed on the continental margin off Southern Chile. Induction vectors observed land-side are presented by Brasse (2009).

unavailable data (note the different period range of the images).

The anomalous responses can be elucidated considering electric and magnetic fields in presence of changing seafloor shape. An enhanced concentration of electrical currents at the continental slope produces anomalous strong vertical magnetic field, that is known also on the land-side as coast effect (e.g., Fischer, 1979). Due to the high sea water conductivity the induced electric currents concentrate primarily in the ocean avoiding the much more resistive subsurface and generate a secondary magnetic field which compensates the primary opposite field, so that the magnetic field diminish considerably or disappears completely in case of insulating substrate as mentioned in 2 and shown in Fig. 2. At the continental margin, where the seafloor shallows towards land, the density of electric currents flowing in the ocean along the coast (i.e. in the TE mode) and above (instead below) measurement points increase inducing an anomalous and opposite magnetic field. This opposite, secondary field becomes predominant on the ocean bottom, where the primary field is strongly damped whereas the electric field is by the coast effect only marginally affected, and causes jumps in the phase (Weidelt, 1994). Moreover the resistivities in TE mode rise steeply generating upward cusps and the tipper gets very large as presented in Fig. 6 and 5.

The periods at which the effects occur depend on position of the probe in relation to the slope and corresponds to lateral distance to which a transfer function is sensitive to bathymetry. However, at high frequencies the field is generally unaffected by the bathymetry and the results are MT-like because the fields still behave like plane waves. At low frequencies, the currents are below the ocean. At the middle frequencies, the currents are in the ocean and this causes the responses looking like those due to infinite line currents right above the station. Note that if the MT responses were recorded on the top of the sea, the responses would be perfectly fine as expected in an usual 2-D case, since all the currents pass below the sounding surface instead above like in the presented marine model. This behavior is overcome or reduced by introducing a very conductive layer below the ocean bottom (e.g., sediments), which has to be at least several kilometers thick. However, the assumption of an oceanic crust being entirely well conductive seems unrealistic; this is even more the case for the continental crust below the slope: every aquiclude would prohibit the intrusion of sea water into deeper layers. Another class of models makes the effect described above disappear too: the association of the upper part of the downgoing plate with a good conductor, in accordance with standard models of subduction.

4 Summary

Offshore magnetotellurics is an useful method for exploration of seafloor and ocean-continent subduction zones, where fluids and melts are known to control the subduction process. A combined on- and offshore magnetotelluric transect across subduction zone is assumed to be able to resolve high conductive structures associated with dehydration processes, water migration and melts building.

However special conditions on the ocean floor not allow to interpret and to deal with the marine records in the same manner as with onshore data. The presence of bathymetry distorts the magnetic and magnetotelluric transfer functions, particularly in the TE mode. Even a gently changing seafloor shape generates an enhanced concentrations of electric currents flowing above instead below measurement station and inducing on the ocean bottom a predominant anomalous opposite magnetic field. This results in phases exceeding the quadrant and cusps in the apparent resistivity.

The high conductive sea water causes a strong attenuation of electric and magnetic field at short periods. Towards long periods the decay differs clearly for both fields. The electric field penetrates the ocean layer from surface to the seafloor, counterintuitive, nearly unchanged, while the magnetic field experiences a strong decay and reaches the ocean bottom just with a fraction of its surface value. Moreover the decay depends strongly from the resistivity contrast between ocean and seafloor. Reducing the resistivity of the basement the electrical thickness of layer increases and both fields approximate a field decay like in a homogeneous half space.

References

Brasse, H., G. Kapinos, Y. Li, L. Mütschard, W. Soyer, D. Eydam (2009): Structural electrical anisotropy in the crust at the South-Central Chilean continental margin as inferred from geomagnetic transfer functions, Phys. Earth Planet. Inter., 173, 7-16.

Brasse, H. (2009): Methods of geoelectric and electromagnetic deep sounding, Lecture Notes, Free University of Berlin.

Chave, A.D., S.C. Constable, and R.N. Edwards (1991): Electrical Exploration Methods for the Seafloor, in: Electromagnetic Methods in Applied Geophysics, Vol. 2 (Ed. M.N. Nabighian), Soc. Expl. Geophys., Tulsa, 931-966.

Constable, S.C., K. Key, and, L. Lewis (2009): Mapping offshore sedimentary structure using electromagnetic methods and terrain effects in marine magnetotelluric data, Geophys. J. Int., 176, 431-442.

Filloux, J.H. (1987):Instrumentation and experimental methods for oceanic studies, in: Geomagnetism, (Eds. J.A. Jacob), Academic Press,1987,143–248.

Fischer, G. (1979): Electromagnetic induction effects on the ocean coast, Proc. IEEE, 67, 1050-1060

McNeill, J.D., and V. Labson (1986), Geological mapping using VLF radio fields. Electromagnetic Methods in Applied Geophysics. Volume 2, Appliction, Parts A and B, (Ed. M.N. Nabighian), SEG, Tulsa, 521-639.

Mackie, R., J. Smith, and T.R. Madden (1994), Three-dimensional modeling using finite difference equations: The magnetotelluric example, Radio Science, 29, 923-935.

Weidelt, P. (1994), Phasenbeziehungen für die B-Polarisation, in: Protokoll über das Kolloquium "Elektromagnetische Tiefenforschung" (Eds. K. Bahr and A. Junge), Höchst, Odenwald, 60-65.